PROCEEDINGS OF SPIE

SPIEDigitalLibrary.org/conference-proceedings-of-spie

Photoacoustic imaging of near-bone soft tissue vasculature in an ex vivo phantom

Guessy Wang, Jeremy M. Hix, Lorenzo Tavelli, Yang Yang

Guessy C. Wang, Jeremy M. L. Hix, Lorenzo Tavelli, Yang Yang, "Photoacoustic imaging of near-bone soft tissue vasculature in an ex vivo phantom," Proc. SPIE 12468, Medical Imaging 2023: Biomedical Applications in Molecular, Structural, and Functional Imaging, 124680A (10 April 2023); doi: 10.1117/12.2653348

SPIE.

Event: SPIE Medical Imaging, 2023, San Diego, California, United States

Photoacoustic Imaging of Near-Bone Soft Tissue Vasculature in an ex vivo Phantom

Guessy C. Wang[a], Jeremy M.L. Hix[b], Lorenzo Tavelli[c], and Yang Yang[d]

[a]Harvard T.H. Chan School of Public Health, Harvard University, 677 Huntington Ave, Boston, United States. [b]Department of Radiology and Institute for Quantitative Health Science and Engineering, Michigan State University, 775 Woodlot Dr, East Lansing, United States. [c]Oral Medicine, Infection, and Immunity, Harvard School of Dental Medicine, Harvard University, 188 Longwood Avenue, Boston, United States. [d]Department of Computational Mathematics, Science and Engineering, Michigan State University, 428 S Shaw Lane, East Lansing, United States.

ABSTRACT

Photoacoustic imaging is an emerging preclinical modality that uses a combination of optics and acoustics mechanisms to visualize differences in optical absorption in target imaging objects. Photoacoustic imaging is potentially suitable for visualizing vasculature, as the hemoglobin in red blood cells is a prominent heat absorber and therefore serves as a great biomarker. Due to acoustic reflection, diffraction and scattering, photoacoustic imaging is subject to artifacts when the target soft tissue is close to bone. We construct an *ex vivo* phantom featuring vascularized soft tissue near long bone, to facilitate evaluation of photoacoustic images and to enable future research on artifact removal in photoacoustic imaging.

Keywords: photoacoustic, reflection artifacts, ex vivo phantom, vasculature imaging

INTRODUCTION

As a non-radioactive, cost-effective emerging preclinical modality, photoacoustic imaging has demonstrated strong promises to be used as a clinical diagnostic aid, primarily due to its ability to identify tissue-specific biomakers such as hemoglobin. Photoacoustic imaging relies on a combination of optics and acoustics to generate images, and therefore enjoys the benefit of both modalities yet also suffer the limitations. Current research applications of photoacoustic imaging have found success in imaging soft tissues up to 10mm in depth, limited by the penetration capability of optics. Some researchers are looking to expand photoacoustic applications to bone using specialized analysis and algorithms. However, few studies are designated to study photoacoustic imaging of soft tissues that are around bone, in which even though the target tissue is fully accessible for photoacoustic imaging, the presence of bone often introduces artifacts and distortions due to acoustic reflection, diffraction and scattering. In this study, we construct an *ex vivo* phantom to facilitate evaluation of photoacoustic images and to enable future research on artifact removal in photoacoustic imaging. The phantom design provides differentiable contrast in soft tissue vasculature utilizing vascular-rich and vascular-poor tissues with long bone in close proximity. This *ex vivo* phantom is imaged with a research-use photoacoustic imaging equipment, and the obtained images are compared to computational simulations for theoretical validation.

THEORY

The photoacoustic imaging equipment used in this study, MSOT 512 echo (iThera Medical), is capable of producing two types of images: ultrasound images and photoacoustic images, in either handheld imaging mode or chamber imaging mode.

Ultrasound Imaging Mechanism: Ultrasound images represent traditional ultrasound imaging similar to the widely used B-mode ultrasound: ultrasound transducers in the imaging equipment produce ultrasound wave towards the target tissue, and the reflected ultrasound signals from target tissue are collected and focused to

Further author information: (Send correspondence to Dr. Lorenzo Tavelli and Dr. Yang Yang.)
Dr. Lorenzo Tavelli: E-mail: lorenzo_tavelli@hsdm.harvard.edu
Dr. Yang Yang: E-mail: yangy5@msu.edu

Medical Imaging 2023: Biomedical Applications in Molecular, Structural, and Functional Imaging,
edited by Barjor S. Gimi, Andrzej Krol, Proc. of SPIE Vol. 12468, 124680A
 · 1605-7422 · doi: 10.1117/12.2653348

produce an image of the target tissue. Ultrasound images can capture a variety of soft tissue structures as they are not tissue specific (aka all soft tissue structures will show on ultrasound image). When bone is present, ultrasound imaging captures the surface of bone without further penetration into bone, and generates artifacts and distortions due to ultrasound wave reflection, diffraction and scattering at the bone surface.

Photoacoustic Imaging Mechanism: Photoacoustic image formation relies on both optics and acoustic imaging mechanisms: Low energy laser pulses in the near infrared spectral range (600–900 nm) are used to shine at the target tissue. The light energy is absorbed by biological pigments (such as hemoglobin, Hb) resulting in heat expansion followed by emission of ultrasound wave. The emitted ultrasound wave is then captured by ultrasound transducers to produce images.[1] Photoacoustic imaging captures only the tissue emitted acoustic waves and therefore is highly tissue-specific (aka only specific tissue type shows on photoacoustic images). Photoacoustic imaging has a penetration depth of 5-10mm due to limited penetration capability of low energy laser light.

Reflection Artifacts due to Presence of Bone: Even though the imaging target is soft tissue, presence of adjacent dense bone can result in artifacts and distortions in photoacoustic images due to acoustic heterogeneity. Specifically, when acoustic wave travels from one medium to another, reflection occurs at the medium interface and the reflected acoustic waves are captured by the transducer as if they are generated from a source, resulting in artifacts or ghost images. These artifacts, known as photoacoustic reflection artifacts, are identified as a major challenge for photoacoustic interpretation, because these artifacts have similar appearances as real image features, resulting in potential misinterpretation.

METHODS

Construction of ex vivo Phantoms: Ex vivo phantom is constructed using fresh crosscut section of bovine femur bone with surrounding muscles and fresh lean chicken. A slice of lean vascular-poor chicken muscle ("the graft") is "transplanted" to a prepared bedding area on the vascular-rich beef muscle near the long bone ("the host"), secured by sutures (Fig. 1). Two experiments were performed with slightly different phantom designs for Phantom 1 and Phantom 2: In Phantom 1, the chicken graft spans through the entire thickness of the phantom, while in Phantom 2, the chicken graft is sandwiched between beef. Phantom 1 was used at after 48 hours of preparation, and Phantom 2 was used at after 12 hours of preparation.

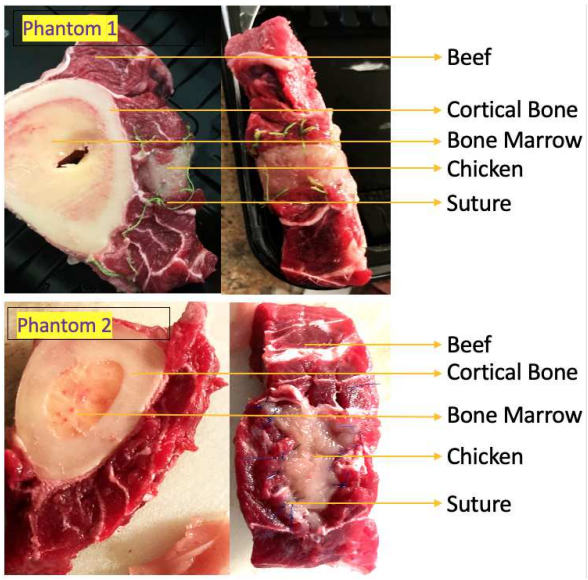

Figure 1. *Ex vivo* phantom construction

Photoacoustic Imaging: The constructed phantoms are then imaged by photoacoustic imaging equipment (MSOT 512 Echo, iThera Medical) to measure hemoglobin readings, using both the handheld imaging mode and the chamber imaging mode. The handheld imaging mode takes one single cross-section image aligned in the middle of the handheld scanner (Fig. 2). Phantom is scanned directly against the scanner with ultrasound gel applied. The chamber imaging mode scans the whole body of the target phantom with 512 transducers located around an arc of 270 degrees, taking a cross section image every 2mm moving along the Z-axis (Fig. 3). Phantoms are wrapped in cellophane wrap with ultrasonic gel on the surface, and immersed fully in water during the imaging process.

Numerical Simulation with Computation Phantom: Computational simulation experiments are constructed using MATLAB k-wave toolbox to identify the artifacts observed in the *ex vivo* study, see Fig. 7. A skinny object with length of 2mm is used as an acoustic source, placed inside "soft tissue" (where sound speed = 1500 m/s) with or without surrounding bone (where sound speed = 3000 m/s).

Figure 2. Handheld imaging mode in MSOT 512 Echo, iThera Medical

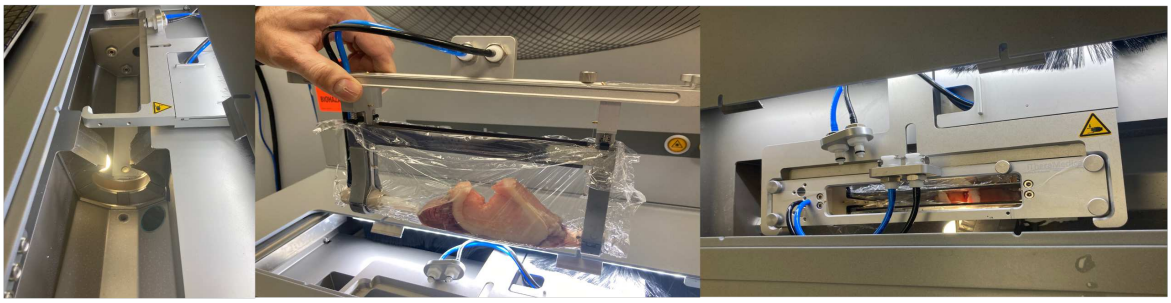

Figure 3. Chamber imaging mode in MSOT 512 Echo, iThera Medical

RESULTS AND DISCUSSIONS

Handheld Images from ex vivo Phantom: Results from handheld imaging mode of Phantom 2 are demonstrated in Fig. 4 and Fig. 5, in which ultrasound images are demonstrated in grey scale, and hemoglobin level is demonstrated in blue in photoacoustic images. As shown in the figures, hemoglobin high regions and low regions correlate well with the location and dimension of vascular-rich beef and vascular-poor chicken, with imaging depth up to 6mm. This correlating pattern was also observed in images from Phantom 1. We also observe artifacts in the region of depth 13mm to 22mm, which is deeper than the region of true images, and that the artifacts have an appearance of reflective image of the true images.

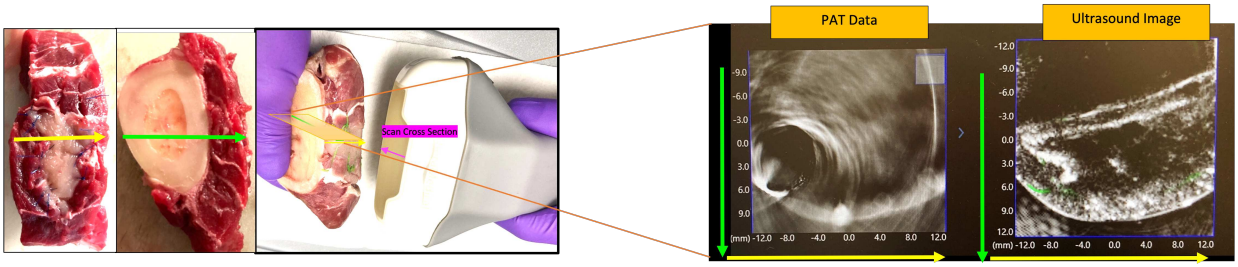

Figure 4. Demonstration of handheld imaging cross-section on *ex vivo* Phantom 2.

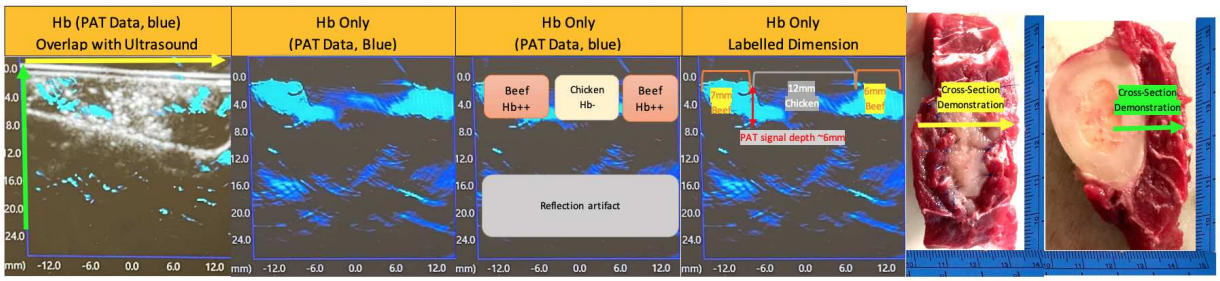

Figure 5. Photoacoustic (PAT) images generated from handheld imaging mode from *ex vivo* Phantom 2.

Chamber Images from ex vivo Phantom: Results from chamber imaging mode of Phantom 1 are demonstrated in Fig. 6. As demonstrated, the phantom scan surface is shown as facing downwards in the photoacoustic image under the chamber imaging mode (which is different from the handheld imaging mode). Image 1, 2 and 3 are cross sections moving along the Z axis (pink), each showing a continuous band of blue signal (high Hb), a lack of blue signal at the bottom centre (low Hb), and again a continuous band of blue signal again (high Hb again), corresponding to the "beef-chicken-beef" pattern on the phantom. The chamber imaging mode proves again that hemoglobin reading on photoacoustic images are correlated to the location and dimension of vascular-rich beef and vascular-poor chicken, with a imaging depth of 4-6mm. A similar artifact at a deeper depth is observed on the chamber imaging mode as well.

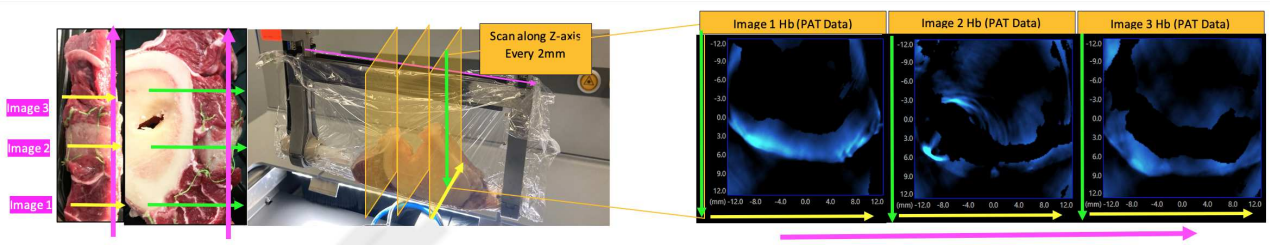

Figure 6. Demonstration of chamber imaging cross-section on *ex vivo* phantom

Numerical Experiment Results: Results from numerical experiment using computation phantom are demonstrated in Fig. 7. The experiment is performed using the MATLAB k-wave toolbox.[2] Fig. 7(a) shows a 2mm source (the ground truth) located in "soft" (sound purple = 1500m/s, purple color), of which the reconstructed image is shown in Fig. 7(b). Fig. 7(c) shows the same 2mm source located in "soft" (sound purple = 1500m/s, purple color) with nearby "bone" (sound speed = 3000m/s, blue color), of which the reconstruction image is shown in Fig. 7(d). As demonstrated, reconstruction image of no bone set up shows no artifact, while reconstruction image of bone adjacent to source shows an artifact at a deeper depth similar to a reflection image. This artifact is similar to what we observed in the *ex vivo* study.

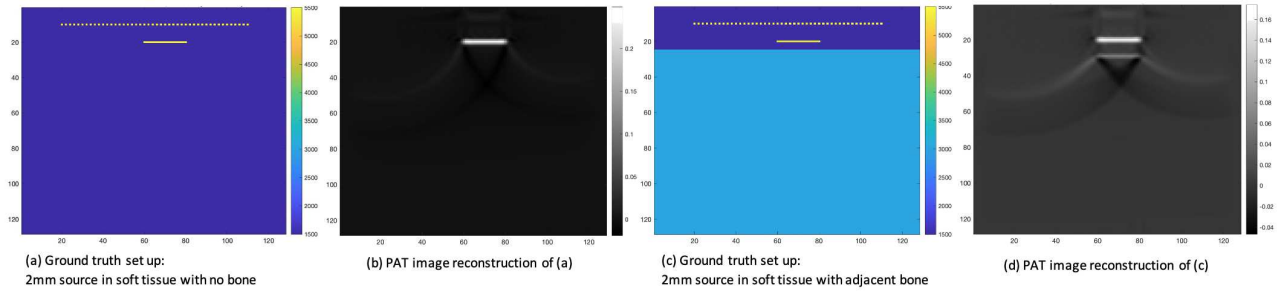

Figure 7. Numerical experiment using computation phantom.

CONCLUSIONS

Photoacoustic images obtained from this *ex vivo* phantom shows high level of hemoglobin reading in regions corresponding to vascular-rich beef, and low level of hemoglobin reading in areas corresponding to vascular-poor chicken, both with good dimension accuracy. It is demonstrated that this *ex vivo* phantom design can serve as an effective photoacoustic phantom with hemoglobin biomarker for evaluating photoacoustic image quality and reconstruction algorithm effectiveness. In addition, the presence of bone in the *ex vivo* phantom provides a biological ground truth that enables future research on artifact removal in photoacoustic imaging. Future direction of our research will explore artifact removal methods in photoacoustic imaging algorithms.[3–11]

ADDITIONAL WORK TO BE PRESENTED

In our current study, the *ex vivo* phantom design and the computational phantom design have different source shapes and different dimensions. We plan to adjust and redo the experiment to use the exact same dimension and experiment setup. We expect the new results will be better suited to demonstrate the artifacts and distortions we observe in both experiments due to the presence of nearby long bone. We expect the study conclusion to be the same or stronger after we obtain new study results.

ACKNOWLEDGMENTS

This research is partly supported by the NSF grant DMS-2006881, NIH grant R03-EB033521, and the startup fund from Michigan State University for Y. Yang. The authors would also like to thank the Institute for Quantitative Health Science & Engineering at Michigan State University for providing access to the photoacoustic imaging equipment iThera MSOT inVision 512-echo.

Results from this research is submitted solely to SPIE Conference Proceeding for Medical Imaging 2023: Biomedical Applications in Molecular, Structural, and Functional Imaging.

REFERENCES

[1] Xia, J., Yao, J., and Wang, L. V., "Photoacoustic tomography: principles and advances," *Progress in electromagnetics research* **147**, 1–22 (2014).

[2] Treeby, B. E. and Cox, B. T., "k-wave: Matlab toolbox for the simulation and reconstruction of photoacoustic wave fields," *Journal of biomedical optics* **15**(2), 021314 (2010).

[3] Allman, D., Reiter, A., and Bell, M. A. L., "Photoacoustic source detection and reflection artifact removal enabled by deep learning," *IEEE transactions on medical imaging* **37**(6), 1464–1477 (2018).

[4] Nguyen, H. N. Y., Hussain, A., and Steenbergen, W., "Reflection artifact identification in photoacoustic imaging using multi-wavelength excitation," *Biomedical optics express* **9**(10), 4613–4630 (2018).

[5] Shan, H., Wang, G., and Yang, Y., "Accelerated correction of reflection artifacts by deep neural networks in photo-acoustic tomography," *Applied Sciences* **9**(13), 2615 (2019).

[6] Singh, M. K. A. and Steenbergen, W., "Photoacoustic-guided focused ultrasound (pafusion) for identifying reflection artifacts in photoacoustic imaging," *Photoacoustics* **3**(4), 123–131 (2015).

[7] Stefanov, P. and Yang, Y., "Multiwave tomography with reflectors: Landweber's iteration," *Inverse Problems & Imaging* **11**(2), 373–401 (2017).

[8] Stefanov, P. and Yang, Y., "Multiwave tomography in a closed domain: averaged sharp time reversal," *Inverse Problems* **31**(6), 065007 (2015).

[9] Vu, T., Li, M., Humayun, H., Zhou, Y., and Yao, J., "A generative adversarial network for artifact removal in photoacoustic computed tomography with a linear-array transducer," *Experimental Biology and Medicine* **245**(7), 597–605 (2020).

[10] Singh, M. K. A., Jaeger, M., Frenz, M., and Steenbergen, W., "In vivo demonstration of reflection artifact reduction in photoacoustic imaging using synthetic aperture photoacoustic-guided focused ultrasound (pafusion)," *Biomedical optics express* **7**(8), 2955–2972 (2016).

[11] Stefanov, P. and Yang, Y., "Thermo-and photoacoustic tomography with variable speed and planar detectors," *SIAM Journal on Mathematical Analysis* **49**(1), 297–310 (2017).